NANO LETTERS

Letter

pubs.acs.org/NanoLett

Switching Individual Quantum Dot Emission through Electrically Controlling Resonant Energy Transfer to Graphene

Jiye Lee,*[,†] Wei Bao,[†,‡] Long Ju,[§] P. James Schuck,[†] Feng Wang,[§] and Alexander Weber-Bargioni*[,†]

[†]Molecular Foundry, Lawrence Berkeley National Laboratory, Berkeley, California 94720, United States

[‡]Department of Materials Science and Engineering and [§]Department of Physics, University of California Berkeley, Berkeley, California 94720, United States

Supporting Information

ABSTRACT: Electrically controlling resonant energy transfer of optical emitters provides a novel mechanism to switch nanoscale light sources on and off individually for optoelectronic applications. Graphene's optical transitions are tunable through electrostatic gating over a broad wavelength spectrum, making it possible to modulate energy transfer from a variety of nanoemitters to graphene at room temperature. We demonstrate photoluminescence switching of individual colloidal quantum dots by electrically tuning their energy transfer to graphene. The gate dependence of energy transfer modulation confirms that the transition occurs when the Fermi level is shifted over half the emitter's excitation energy. The modulation magnitude decreases rapidly with increasing emitter−graphene distance (d), following the $1/d^4$ rate trend unique to the energy transfer process to two-dimensional materials.

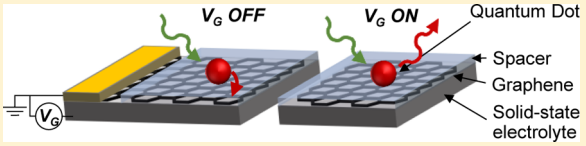

KEYWORDS: *Resonant energy transfer, graphene, colloidal quantum dots, FRET, nanophotonic switch*

Nanoemitters, such as epitaxial and colloidal quantum dots and organic dyes, are essential building blocks for quantum optics, nanophotonic communication and biological imaging.[1,2] Electrical control of individual nanoscale photon sources may inspire the development of novel functions in optoelectronic applications: e.g., nanoscale optical switches smaller than the light diffraction limit. For their practical, widespread use, electrically tunable nanoemitter switches need to be able to operate at room temperature and integrate a diverse type of light-emitting nanomaterials, including solution-processable materials, with various bandgaps.

Switching semiconductor quantum dots on and off with voltages has been previously realized by incorporating them into a p-i-n diode, leading to electrically driven single photon sources.[3] However, this top-down fabrication approach is limited only for epitaxial quantum dots and inapplicable for solution-processable emitters, which are attractive due to their inexpensive synthesis and processing and biocompatibility. One way to electrically control the local light emission of soluble nanomaterials is to modulate Förster energy transfer from a donor to an acceptor.[4] Becker et al. demonstrated that the efficiency of energy transfer from a donor rod-like semiconductor nanocrystal to an acceptor dye can be varied by voltage using the nanocrystal's quantum-confined Stark effect (QCSE), turning on and off the emission from either the dye molecule or the nanocrystal.[4] In this approach, however, the optical transition line width should be narrower than the QCSE shift, which is up to tens of meV,[5,6] limiting the operation to liquid-nitrogen temperature. Also, as the inhomogeneous broadening of the quantum dot's bandgap is larger than the QCSE shift, only certain donor−acceptor pairs with highly similar energies are switchable.

Compared with relatively weak QCSE in zero-dimensional quantum dots, graphene, a single layer of hexagonally arranged carbon atoms, exhibits an unusually strong change in optical transitions under electrical gating.[7,8] By changing the carrier concentrations through electrostatic doping, the Fermi level (E_F) of graphene can be varied. The electron filling of the conduction band or the electron depletion of the valence band blocks the interband transitions with energy below $2|E_F|$. Gate-tunable optical transitions of graphene have been demonstrated for visible and infrared wavelengths and applied to various types of optoelectronic devices,[9] including broadband electro-optic modulators,[10−12] photonic crystal cavity,[13] and tunable infrared plasmonic devices.[14−17] Here we employ gate-variable optical response in graphene to electrically control resonant energy transfer from colloidal quantum dots to graphene. The broadband modulation of optical transitions in graphene allows photoluminescence switching of quantum dots with different bandgaps at room temperature.

Figure 1 illustrates the mechanism to control nonradiative energy transfer through electrostatic doping of graphene. With no gate voltage (V_G) applied, the Fermi level lies around the Dirac point and an electron in the valence band can be excited by resonant energy transfer from a localized emitter situated within tens of nanometers (Figure 1a). This energy transfer process to graphene has been experimentally demonstrated for a variety of emitters: semiconductor nanocrystals,[18−20] dye molecules,[21,22] and diamond nitrogen vacancies.[23,24] When the Fermi level is raised over half the emitter's excitation energy

Received: September 17, 2014
Revised: November 6, 2014
Published: November 10, 2014

   dx.doi.org/10.1021/nl503587z | *Nano Lett.* 2014, 14, 7115−7119

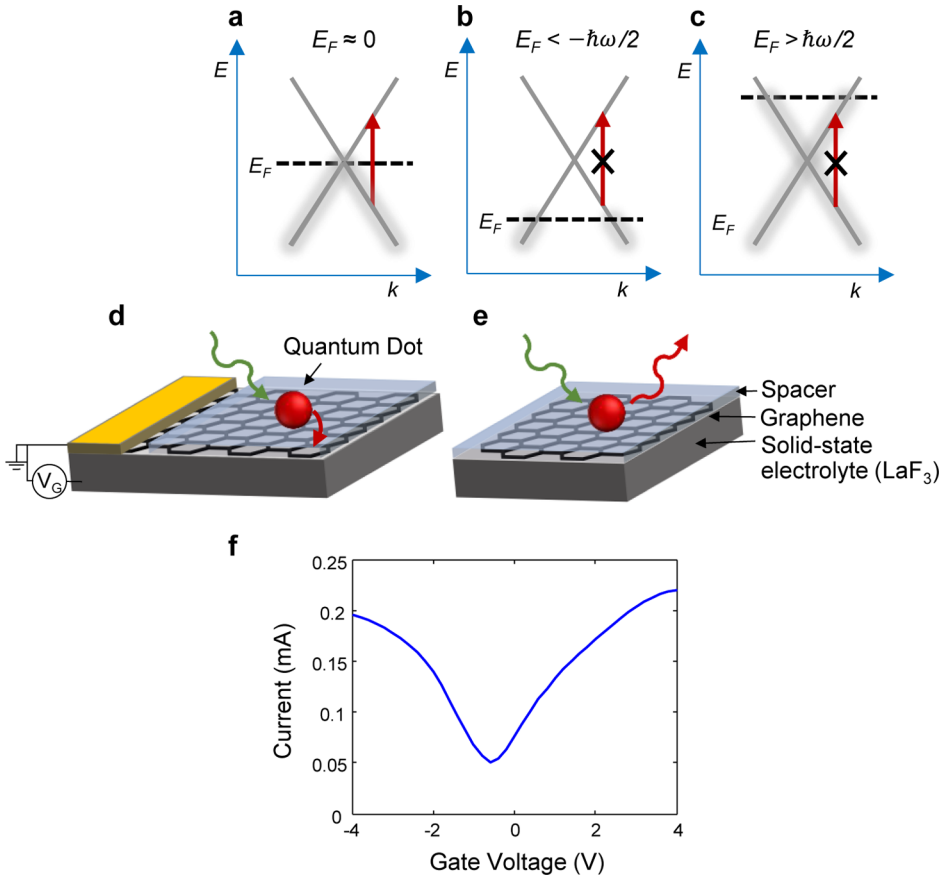

Figure 1. Operation mechanism of electrically controllable energy transfer from quantum dots to graphene. (a,b,c) Graphene's band structures at different gate voltages (V_G). At $V_G = 0$ (a), the Fermi level (E_F) of graphene stays near the Dirac point and electrons can be photoexcited. When the application of a gate bias lowers the Fermi level below half the quantum dot's exciton energy (b), depletion of electrons disallows the interband transitions. When the Fermi level is shifted above half the exciton energy (c), the electron filling of the conduction band forbids the optical transition. (d,e) Device structure and illustration of energy transfer when V_G is off (d) and on (e). The graphene sheet was gated with LaF_3, a solid-state electrolyte, and covered with a thin PMMA spacer layer. At $V_G = 0$, PbS colloidal quantum dots show energy transfer to graphene. When a gate voltage is applied to shift the Fermi energy (such as in panel b or c), the energy transfer is suppressed and the quantum dots emit photons to free space. (f) Source-drain current of a graphene transistor gated by LaF_3 as a function of gate voltage. The source-drain voltage was 0.1 V over a 20 μm wide, 20 μm long channel.

(i.e., $E_F > \hbar\omega/2$), the arrival state for electron excitation is already occupied, disallowing the interband transition (Figure 1c). Lowering the Fermi level by more than half the emitter energy results in the depletion of electrons necessary for excitation, forbidding the optical transition (Figure 1b). The carrier doping dependence of Förster-like energy transfer to graphene has been theoretically studied in refs 25−27. Electrically tunable energy transfer to graphene allows us to turn the luminescence of nanoemitters on and off.

To test the effect of electrostatic doping on resonant energy transfer to graphene, we fabricated the device structure shown in Figure 1d,e. The graphene layer was back-gated with lanthanum fluoride (LaF_3), a solid-state electrolyte.[28] LaF_3 is an ionic conductor at room temperature where the mobile carriers are fluorine ion vacancies.[28] Like liquid or ion-gel electrolytes previously employed to gate graphene,[13,29] LaF_3 can induce larger electrostatic doping than dielectric oxides. A LaF_3 film forms a thin dipole layer at its surface that produces a large capacitance, which can be effectively treated as that of a 10−20 nm thick insulating layer (independent of the actual film thickness) with a dielectric constant of 14.[28] This work assumed 10 nm for the insulator's effective thickness. Graphene was covered with a thin film of insulating poly(methyl methacrylate) (PMMA) with varying thicknesses. Finally, lead sulfide (PbS) colloidal quantum dots with the photon emission energy of ∼0.9 and ∼1.3 eV were chosen as the emitter; see Figure S1 in Supporting Information for their photoluminescence spectra. See the Methods section for the detailed description on device structures and fabrication.

Figure 2 shows electrical switching of photoluminescence of individual PbS quantum dots capped with cadmium sulfide (CdS) shells emitting at 1.3 eV; see the Methods section for the procedure to take photoluminescence micrographs. To improve the signal-to-noise ratio, we imaged a cluster of a couple of nanocrystals rather than a single particle. The peak photoluminescence intensity at $V_G = -5$ V increased by ∼50% compared to $V_G = 0$ V. The Fermi level shift (E_F) is determined by $E_F = \hbar\nu_F(\pi n)^{1/2}$, where $\hbar$ is Planck's constant, ν_F is the Fermi velocity (1×10^6 m s^{-1}), and n is the carrier density.[7] According to this relationship, a gate voltage over 4 V is required to bring the Fermi level above the transition threshold ($E_F = \hbar\omega/2$). Quantum dots on a bare LaF_3 substrate without graphene showed no photoluminescence modulation.

Figure 3 displays the gate dependence of the photoluminescence intensity for PbS and PbS/CdS nanocrystals emitting at 0.9 and 1.3 eV, respectively. As expected, the 1.3 eV

dx.doi.org/10.1021/nl503587z | Nano Lett. 2014, 14, 7115−7119

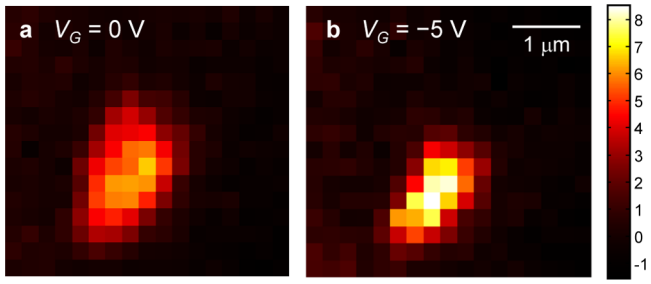

Figure 2. Electrical switching of photoluminescence of individual quantum dots. (a) Photoluminescence intensity map of individual PbS/CdS quantum dots emitting at 1.3 eV at a gate voltage (V_G) of 0 V. (b) The equivalent of panel a at V_G = −5 V. The background emission of LaF_3 was subtracted for clarity. The PMMA spacer was 5 nm thick.

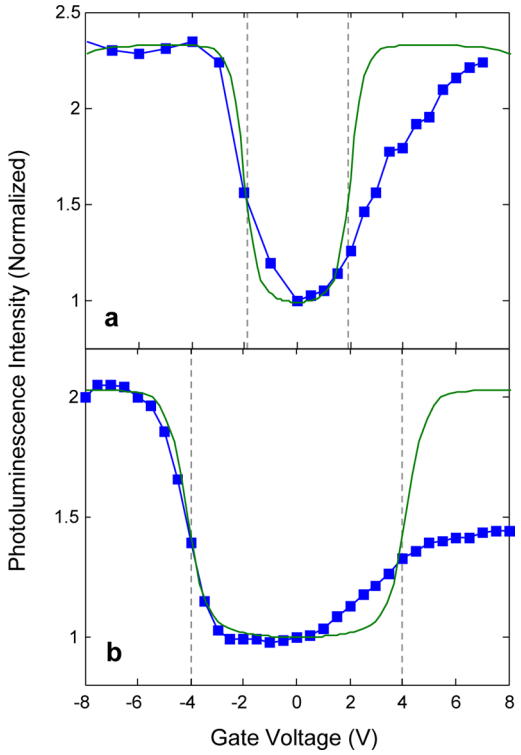

Figure 3. Voltage dependence of energy transfer. (a) Modulation of photoluminescence intensity (■) at different gate voltages (V_G) for PbS nanocrystals emitting at 0.9 eV. (b) The equivalent of panel a for PbS/CdS nanocrystals emitting at 1.3 eV. The photoluminescence intensity was normalized to V_G = 0 V. The PMMA spacer was 3 nm thick. The simulated photoluminescence (solid green) was obtained by calculating the energy transfer rate from quantum dots to graphene. The dotted lines represent the gate voltage at which the Fermi level shift is half the quantum dot's exciton energy.

nanocrystals need higher voltages for switching than the 0.9 eV nanocrystals; the dotted lines in Figure 3 show the gate voltage at the transition threshold ($E_F = \hbar\omega/2$). The overall photoluminescence yield of nanocrystals is $\Gamma_r/(\Gamma_r + \Gamma^i_{nr} + \Gamma^g_{nr})$, where Γ_r, Γ^i_{nr}, and Γ^g_{nr} are the rates of radiative decay, intrinsic nonradiative recombination, and energy transfer to graphene, respectively. Previous studies showed in the case of colloidal quantum dots,[18] dye molecules,[21] and diamond nitrogen vacancies[23] that the energy transfer rate to graphene without voltage can be greater than the radiative rate by up to 2 orders of magnitude. When the Fermi level rises over half the photon energy, the optical conductivity of graphene from the interband transition drops from $e^2/4\hbar$ to nearly zero.[29] Consequently, the resonant energy transfer process to graphene becomes insignificant compared to radiative decay ($\Gamma^g_{nr} < \Gamma_r$) and the photoluminescence efficiency approaches that without graphene. Further increase in the Fermi level over the emitter's exciton energy ($|E_F| > \hbar\omega$) leads to excitation of surface plasmons, electromagnetic waves propagating along the interface between highly doped graphene and a dielectric.[14,17] However, at the doping level where our device operates ($0 < |E_F| < \hbar\omega$), the decay into the plasmons is considerably smaller than interband transitions.

To simulate our experiment results, among a few theoretical studies that model the doping dependence of energy transfer to graphene,[25−27,30] we followed the work by Koppens and coworkers.[25] The energy transfer rate can be predicted by calculating the coupling between the transition dipole and the induced electromagnetic modes acting on itself; see ref 25 or Supporting Information. When taking into account the thermal effect in graphene's optical absorption (see Supporting Information), the simulation reproduced the gradual voltage-dependent change in photoluminescence intensity. Γ^i_{nr} was assumed to be 90 and 300 times Γ_r for the 1.3 and 0.9 eV nanocrystals, respectively. We note that since the on/off switching ratio is determined by the competition between intrinsic decays ($\Gamma_r + \Gamma^i_{nr}$) and energy transfer to graphene (Γ^g_{nr}), high-quantum-efficiency quantum dots with small Γ^i_{nr} are expected to show stronger modulation; a quantum dot with a unity photoluminescence yield may show the on/off ratio larger than 100. Some devices exhibited the asymmetric photoluminescence−intensity−voltage characteristics as shown in Figure 3b, which are likely due to the effect of doping produced during graphene growth or transfer,[31] as they resemble the asymmetric gate dependence of current observed in those graphene transistors (see Figure S2 in Supporting Information).

As shown in Figure 4, the modulation of energy transfer depends on the distance between the emitter and the graphene

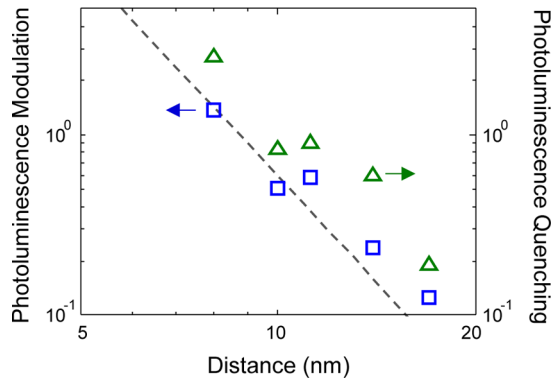

Figure 4. Photoluminescence modulation and quenching as a function of quantum dot−graphene distance (d). The photoluminescence modulation (□) and quenching (△) factors are set to be proportional to the rate of resonant energy transfer. The modulation factor is the difference between the maximum photoluminescence intensity during the voltage sweep and the intensity at V_G = 0, normalized to V_G = 0. The quenching factor is the difference between the photoluminescence intensity with and without graphene, normalized to that with graphene. The modulation and quenching factors were modeled (dotted line) by calculating the energy transfer rate, which scales as d^{-4}.

dx.doi.org/10.1021/nl503587z | Nano Lett. 2014, 14, 7115−7119

sheet (d). The PMMA spacer thickness was adjusted to vary the separation. Additional 5 nm was added to the distance, taking into account the length of nanocrystal ligands (~2 nm) and the radius of the nanocrystal (~3 nm). The photoluminescence modulation and quenching factors are defined to be proportional to the energy transfer rate; both factors are $\sim\Gamma_{nr}^{g}/(\Gamma_r + \Gamma_{nr}^{i})$ (see Supporting Information for derivation). The modulation factor is the difference between the maximum and minimum photoluminescence intensities during the voltage sweep, and the quenching factor is the photoluminescence intensity quenched by graphene compared to the intensity on a LaF_3 substrate; see Figure 4 caption about normalization. Although the simulation indicates that energy transfer to graphene with sufficient voltages should become significantly slower than the other competing processes, we observed that the photoluminescence under gating does not recover fully up to the status without graphene. The discrepancy between the modulation and quenching factors may be because direct charge transfer occurs in the region that a spacer layer covers incompletely or some part of the graphene sheet includes impurity or graphene crystal boundaries, which could quench nanocrystal excitons in spite of gate bias.

In a typical Förster resonance transfer process between two point dipoles, the rate scales as d^{-6}.[32] In contrast, resonant energy transfer from a zero-dimensional emitter to two-dimensional lossy media (e.g., graphene) follows the rate scaling of d^{-4}. Previous studies predicted and experimentally demonstrated the d^{-4} dependence of fluorescence quenching by graphene.[21,23,33,34] Furthermore, the energy transfer rate can be described only as a function of donor−acceptor distance and universal parameters (including the fine structure constant $\alpha = e^2/\hbar c$), independent of material specifics.[21,23,33] Both our modulation and quenching measurements qualitatively agree with the simulated rate of energy transfer, which follows the d^{-4} dependence, confirming the previous experimental observations for organic molecules[21] and diamond nitrogen vacancies.[23]

We demonstrated electrical switching of nanoemitters by varying their energy transfer to graphene. The nanoemitter switch can be built as small as tens of nanometers, making it one of the smallest light modulation devices; this potentially allows control of light emission beyond the diffraction limit and superb switching speed, which is only limited by spontaneous emission of optical emitters due to elimination of RC delays.[13] Furthermore, this graphene/nanoemitter hybrid device can be easily integrated with optical nanoantenna, which can enhance the rate[35] or modify the direction[36] for photon emission. Powered by these benefits, graphene-based nanoemitter modulators shown here are expected to become enabling technologies in nanophotonic communication, quantum optics, and optical detection and interrogation of biological systems.

Methods. *Device Fabrication.* A single-crystal LaF_3 substrate with (100) orientation (MTI Corporation) was used as a solid-state electrolyte for gating. Monolayer graphene on copper foils was purchased from ACS Material or grown by chemical vapor deposition independently. After PMMA was spin-coated on graphene, copper foils were etched by ammonium persulfate solution (0.1 M). Graphene was transferred to a LaF_3 substrate and the PMMA layer was dissolved by acetone. The graphene layer was patterned by photolithography, followed by reactive ion etching in oxygen. Gold electrodes with a chromium adhesion layer were defined using photolithography and thermal evaporation. Graphene was covered by spin-coated PMMA. We spin-coated PbS nanocrystals (Evident Technologies) in hexane/octane (9:1) mixture or PbS/CdS nanocrystals (NanoOptical Materials) in hexane. The concentration of the solution was adjusted to produce roughly a monolayer of nanocrystals for the measurements reported in Figures 3 and 4. The solution was diluted to yield individual quantum dots for the experiment in Figure 2. A gold pad was used to bias a LaF_3 substrate.

Photoluminescence Measurement. A diode-pumped solid-state laser at λ = 532 nm photoexcited nanocrystals through a microscope objective. The laser power was ~1200 W/cm^2 (for Figure 2) and ~500 W/cm^2 (for Figures 3 and 4), low enough so that the photoluminescence intensity is linearly proportional to the excitation power. The photoluminescence of 0.9 eV-emitting PbS and 1.3 eV-emitting PbS/CdS nanocrystals was collected by an InGaAs photodetector and a Si avalanche photodiode, respectively. The photoluminescence micrograph (Figure 2) was obtained by collecting fluorescence through a 100× microscope objective with a Si avalanche photodiode while moving a sample with a piezoelectrically controlled stage.

Modeling Parameters. The relative permittivity of LaF_3 and PMMA is 2.56[37] and 2.22,[38] respectively.

■ ASSOCIATED CONTENT

Supporting Information

Description of a model for energy transfer from an emitter to graphene; fluorescence spectra of PbS colloidal quantum dots; asymmetric current−voltage characteristics of a graphene transistor. This material is available free of charge via the Internet at http://pubs.acs.org.

■ AUTHOR INFORMATION

Corresponding Authors

*E-mail: jiyelee@lbl.gov.
*E-mail: awb@lbl.gov.

Notes

The authors declare no competing financial interest.

■ ACKNOWLEDGMENTS

Work at the Molecular Foundry was supported by the U.S. Department of Energy (DOE), Office of Basic Energy Sciences, Scientific User Facilities Division, under contract no. DE-AC02-05CH11231. The device fabrication was supported by the Laboratory Directed Research and Development (LDRD) funding from Berkeley Lab, provided by the Director, Office of Science, of the U.S. Department of Energy under contract no. DE-AC02-05CH11231. The analysis was supported by the U.S. Department of Energy, Office of Science, Basic Energy Sciences, Scientific User Facilities Division (NSRCs) Early Career Award. We thank April Sawvel for help with colloidal quantum dots and Hsin-Zon Tsai, Han-Sae Jung, Xuefei Feng, and Prof. Michael Crommie for support with graphene growth and transfer.

■ REFERENCES

(1) Jahnke, F. *Quantum Optics with Semiconductor Nanostructures*; Elsevier: New York, 2012.
(2) Zrazhevskiy, P.; Sena, M.; Gao, X. *Chem. Soc. Rev.* **2010**, *39* (11), 4326−4354.
(3) Yuan, Z.; Kardynal, B. E.; Stevenson, R. M.; Shields, A. J.; Lobo, C. J.; Cooper, K.; Beattie, N. S.; Ritchie, D. A.; Pepper, M. *Science* **2002**, *295* (5552), 102−105.
(4) Becker, K.; Lupton, J. M.; Muller, J.; Rogach, A. L.; Talapin, D. V.; Weller, H.; Feldmann, J. *Nat. Mater.* **2006**, *5* (10), 777−781.

(5) Müller, J.; Lupton, J. M.; Lagoudakis, P. G.; Schindler, F.; Koeppe, R.; Rogach, A. L.; Feldmann, J.; Talapin, D. V.; Weller, H. *Nano Lett.* **2005**, *5* (10), 2044−2049.
(6) Empedocles, S. A.; Bawendi, M. G. *Science* **1997**, *278* (5346), 2114−2117.
(7) Wang, F.; Zhang, Y.; Tian, C.; Girit, C.; Zettl, A.; Crommie, M.; Shen, Y. R. *Science* **2008**, *320* (5873), 206−209.
(8) Li, Z. Q.; Henriksen, E. A.; Jiang, Z.; Hao, Z.; Martin, M. C.; Kim, P.; Stormer, H. L.; Basov, D. N. *Nat. Phys.* **2008**, *4* (7), 532−535.
(9) Bao, Q.; Loh, K. P. *ACS Nano* **2012**, *6* (5), 3677−3694.
(10) Liu, M.; Yin, X.; Ulin-Avila, E.; Geng, B.; Zentgraf, T.; Ju, L.; Wang, F.; Zhang, X. *Nature* **2011**, *474* (7349), 64−67.
(11) Youngblood, N.; Anugrah, Y.; Ma, R.; Koester, S. J.; Li, M. *Nano Lett.* **2014**, *14* (5), 2741−2746.
(12) Koester, S. J.; Li, M. *Appl. Phys. Lett.* **2012**, *100* (17), 171107.
(13) Majumdar, A.; Kim, J.; Vuckovic, J.; Wang, F. *Nano Lett.* **2013**, *13* (2), 515−518.
(14) Chen, J.; Badioli, M.; Alonso-Gonzalez, P.; Thongrattanasiri, S.; Huth, F.; Osmond, J.; Spasenovic, M.; Centeno, A.; Pesquera, A.; Godignon, P.; Zurutuza Elorza, A.; Camara, N.; de Abajo, F. J. G.; Hillenbrand, R.; Koppens, F. H. L. *Nature* **2012**, *487*, 77−81.
(15) Yao, Y.; Kats, M. A.; Genevet, P.; Yu, N.; Song, Y.; Kong, J.; Capasso, F. *Nano Lett.* **2013**, *13* (3), 1257−1264.
(16) Yao, Y.; Kats, M. A.; Shankar, R.; Song, Y.; Kong, J.; Loncar, M.; Capasso, F. *Nano Lett.* **2013**, *14* (1), 214−219.
(17) Fei, Z.; Rodin, A. S.; Andreev, G. O.; Bao, W.; McLeod, A. S.; Wagner, M.; Zhang, L. M.; Zhao, Z.; Thiemens, M.; Dominguez, G.; Fogler, M. M.; Neto, A. H. C.; Lau, C. N.; Keilmann, F.; Basov, D. N. *Nature* **2012**, *487* (7405), 82−85.
(18) Chen, Z.; Berciaud, S.; Nuckolls, C.; Heinz, T. F.; Brus, L. E. *ACS Nano* **2010**, *4* (5), 2964−2968.
(19) Ajayi, O. A.; Anderson, N. C.; Cotlet, M.; Petrone, N.; Gu, T.; Wolcott, A.; Gesuele, F.; Hone, J.; Owen, J. S.; Wong, C. W. *Appl. Phys. Lett.* **2014**, *104* (17), 171101.
(20) Dong, H.; Gao, W.; Yan, F.; Ji, H.; Ju, H. *Anal. Chem.* **2010**, *82* (13), 5511−5517.
(21) Gaudreau, L.; Tielrooij, K. J.; Prawiroatmodjo, G. E. D. K.; Osmond, J.; de Abajo, F. J. G.; Koppens, F. H. L. *Nano Lett.* **2013**, *13* (5), 2030−2035.
(22) Kim, J.; Cote, L. J.; Kim, F.; Huang, J. *J. Am. Chem. Soc.* **2009**, *132* (1), 260−267.
(23) Tisler, J.; Oeckinghaus, T.; Stöhr, R. J.; Kolesov, R.; Reuter, R.; Reinhard, F.; Wrachtrup, J. *Nano Lett.* **2013**, *13* (7), 3152−3156.
(24) Stöhr, R. J.; Kolesov, R.; Xia, K.; Reuter, R.; Meijer, J.; Logvenov, G.; Wrachtrup, J. *ACS Nano* **2012**, *6* (10), 9175−9181.
(25) Koppens, F. H. L.; Chang, D. E.; García de Abajo, F. J. *Nano Lett.* **2011**, *11* (8), 3370−3377.
(26) Nikitin, A. Y.; Guinea, F.; Garcia-Vidal, F. J.; Martin-Moreno, L. *Phys. Rev. B* **2011**, *84* (19), 195446.
(27) Swathi, R.; Sebastian, K. *J. Chem. Sci.* **2012**, *124* (1), 233−240.
(28) Sher, A.; Miller, W. E.; Tsuo, Y. H.; Moriarty, J. A.; Crouch, R. K.; Seiber, B. A. *Appl. Phys. Lett.* **1979**, *34* (11), 799−801.
(29) Chen, C.-F.; Park, C.-H.; Boudouris, B. W.; Horng, J.; Geng, B.; Girit, C.; Zettl, A.; Crommie, M. F.; Segalman, R. A.; Louie, S. G.; Wang, F. *Nature* **2011**, *471* (7340), 617−620.
(30) Velizhanin, K. A.; Efimov, A. *Phys. Rev. B* **2011**, *84* (8), 085401.
(31) Wang, H.; Wu, Y.; Cong, C.; Shang, J.; Yu, T. *ACS Nano* **2010**, *4* (12), 7221−7228.
(32) Förster, T. *Ann. Phys.* **1948**, *437* (1−2), 55−75.
(33) Swathi, R. S.; Sebastian, K. L. *J. Chem. Phys.* **2009**, *130* (8), 086101.
(34) Gómez-Santos, G.; Stauber, T. *Phys. Rev. B* **2011**, *84* (16), 165438.
(35) Kinkhabwala, A.; Yu, Z.; Fan, S.; Avlasevich, Y.; Mullen, K.; Moerner, W. E. *Nat. Photonics* **2009**, *3* (11), 654−657.
(36) Curto, A. G.; Volpe, G.; Taminiau, T. H.; Kreuzer, M. P.; Quidant, R.; van Hulst, N. F. *Science* **2010**, *329* (5994), 930−933.
(37) Bennett, H. E. *Laser Induced Damage in Optical Materials, 1982: Proceedings of a Symposium*; US Dept. of Commerce, National Bureau of Standards: Gaithersburg, MD, 1984; Vol. *847*.
(38) Kasarova, S. N.; Sultanova, N. G.; Ivanov, C. D.; Nikolov, I. D. *Opt. Mater.* **2007**, *29* (11), 1481−1490.